Phys. 235 Lecture Notes - Week 7

Lecture by: P. H. Diamond, Notes by: R. J. Hajjar

June 1, 2016

1 Hurst exponent, fractal dimensions and time series

So far we covered the topic of intermittency as a concentration of probability distribution function in localized small patches. We also introduced time series as a collection of experimental data obtained over a certain time range t or at different number of steps N. Investigating the variance and other subsequent moments of such a series provides qualitative insight on the dynamical behavior of the system that generated this data.

The classic example of a time series discussed in class was the Nile flooding and the associated intermittent Joseph and Noah effects. The two terms were introduced by Mandelbrot to describe the memory of a time series. By definition, the Joseph effect describes movements that are part of a larger, overall stationary cycle yet presents patterns of high and low amplitude respectively (7 years of famine followed by 7 years of abundance Joseph talked about in the Old testament) and the Noah effect is associated with large and amplified rare events that lead to infinite variance in the series (the great flood).

The topic of time series lead us to define the Hurst exponent of a random process $B(t)$ as a parameter that encodes the fractal character of the dynamics behind the series:

$$D \sim \frac{log(N)}{log(1/\epsilon)} \rightarrow H \sim \frac{log(\Delta B)}{log(\Delta t)}$$

suggesting a direct relation to the fractal dimension and to the degree of randomness in the series (mild, wild or slow randomness). Here ΔB and Δt are increments over a non vanishing interval. A direct relation between H and D is:

$$H = 2 - D$$

where $1 < D < 2 \rightarrow 0 < H < 1$. This direct relation between H and D implies that the Hurst exponent is a measure of the fractal smoothness based
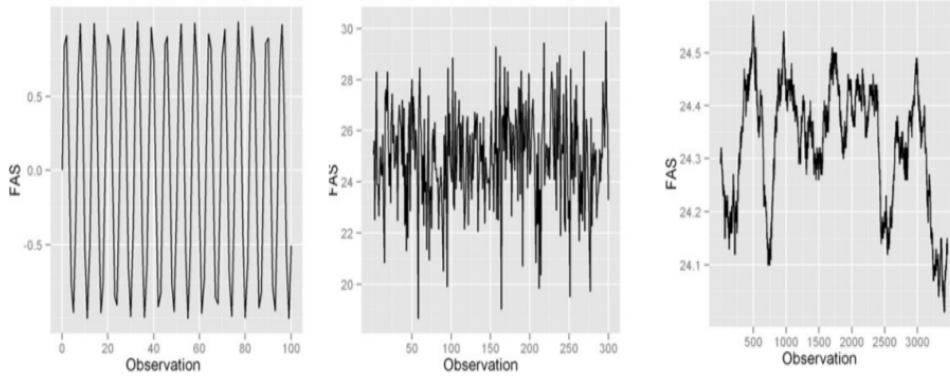
Figure 1: Examples of data series for values of the Hurst exponent $H = 0.043$, $H = 0.53$ and $H = 0.95$ respectively.

on the asymptotic behavior of the rescaled range of the time process. Hurst exponent satisfies the equation:

$$\delta^{2H} = \frac{R(\delta)}{S(\delta)}$$

where δ is equivalent to time, $R(\delta)$ is the statistical data range and $S(\delta)$ is the standard deviation of the statistical set. In this sense, H is the counterpart of fractal dimension for intermittency in time series. Depending on the value of H, the series can be classified into different types and consequently exhibits different behaviors (See Fig. 1):

For $0 < H < 0.5$: the time series switches or alternates between high and low values. The parameter in question increases and decreases in an anti persistent oscillatory motion, exhibiting a higher than normal order of randomness with a tendency to regress to the mean.

For $0.5 < H < 1$ there is a persistent trend or pattern in the data. A sense of long memory affects the system behavior and influences its later dynamics pushing for the parameter in question to stick to its previous value as time passes and as the series evolves.

The $H = 0.5$ case corresponds to an ordinary Weiner Brownian diffusive motion (Central limit theorem).

At this point, one might ask the question: how is this related to plasmas? Clearly, an analogy between the Nile example and a plasma confinement system can be drawn, that is:

	Nile flooding example	Plasma system
Source	rain	input power
Stock system	water reservoir level	plasma energy
Transport to stock system	river	plasma transport mechanism
Transport out of stock system	pipe	outflow flux

Fig.(2) helps illustrating the analogy furthermore:
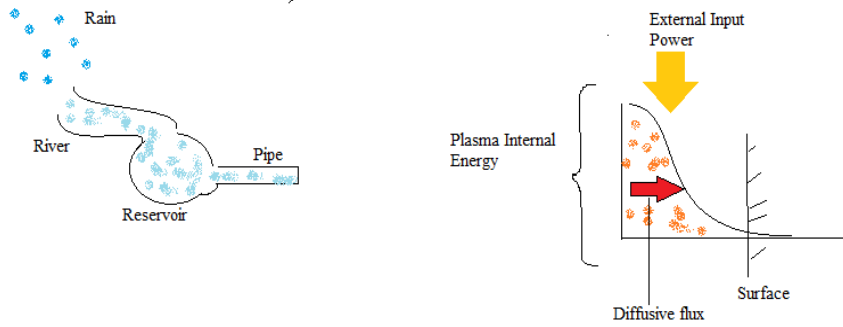
Figure 2: Analogy between the Nile example and a plasma confinement system.

2 How to extract H from a time series?

Given a time series, the first oder of business is to figure out a way to compute the Hurst exponent H of the series in order to properly characterize the data set. For a data set $X_1, X_2, \ldots X_n$, we define the expectation value:

$$E[\frac{R(n)}{S(n)}] = Cn^{2H}$$

where n is a number of points, $S(n)$ and $R(n)$ are the standard deviation and the range of the series containing the first n values spanned in time. The procedure is to divide the original n-terms series into subsets or sub-series for each $n = [N, N/2, N/4 \ldots]$, then for each constructed time subset:

- Calculate the mean $m = \frac{1}{n} \sum_{i=1}^{n} X_i$

- Adjust the series to the mean by setting $Y_t = X_t - m$ for $t = 1, \ldots n$

- Compute the cumulative deviation from the mean $Z_t = \sum_{i=1}^{t} Y_i$

- Compute the *range of deviation* $R = max(Z_1, \ldots Z_n) - min(Z_1, \ldots Z_n)$

- Compute the *standard deviation* $S(n) = (\frac{1}{n} \sum_{n=1}^{n} (X_i - m)^2)^{1/2}$

From the average ratio $\overline{R(n)/S(n)}$, H can be calculated as the range of cumulative deviation over the standard deviation of the series:

$$\frac{\overline{R(n)}}{S(n)} = Cn^{2H}$$

Here the average is performed over all partial time series, which are subsets of the original n-terms time series. For $H > 0.5$ the future trend of the time series will be consistent with its past, for $H < 0.5$, it evolves in an opposite trend and for $H = 0.5$ the future of the series is random.

For the Nile example, the empirical value of H lies between 0.7 and 0.8 as measured by H. E. Hurst. Clearly $H \neq 0.5$ and the time series of the river water level does not fit a Gaussian distribution. It shows instead characteristics of discontinuity and durability i.e. the Noah and the Joesph effects respectively. Random Brownian models cannot be used to describe this so called fractional Brownian motion (FBM). The expectation of the first and the second order moments are then:

$$E\{B_H(t + T) - B_H(t)\} = 0$$

$$E\{(B_H(t + T) - B_H(t))^2\} = T^{2H}$$

instead of being:

$$E\{B_H(t + T) - B_H(t)\} = 0$$

$$E\{(B_H(t + T) - B_H(t))^2\} = T$$

where the increment $T > \tau_{ac}$ for a Wiener Brownian motion (WBM). We mention that the above definition can be generalized for a fractal/multi-fractal by a uniscaling property stating that:

$$E\{|B_H(t + T) - B_H(t)|^q\}^{1/q} = Ct \times T^H$$

Cases where the q-th scale factor depends on q are called multi-scales and will be studied in the next section.

3   Properties of a time series spectral density.

When a time series is collected, one would try to investigate its higher order moments to get meaningful insight on its physics. Measurements of the second order moment (variance), the third order moment (skewness) and the fourth order moment (kurtosis) characterize the series tail and flatness. Given a time series $g(t)$, we define a generalized Hurst exponent $H = H(q)$

that is derived from the higher order moments of the series. The expectation value of the q-th order $E\{|B_H(t+T) - B_H(t)|^q\}$ is q dependent since it is a multi-fractal case:

$$E\{|B_H(t+T) - B_H(t)|^q\} \propto f(q)$$

By analogy with turbulence, the correlation function of the data points in the series is:

$$S_q = \langle (g(t+\tau) - g(t)^q) \rangle \sim \tau^{qH(q)}$$

where $t > \tau$, τ being the time lag between two data points. The spectral density can be obtained by computing the frequency spectrum of the auto-correlation function S_q i.e. computing its Fourier transform:

$$\langle B^2 \rangle_w = \int e^{-iw\tau} \langle \Delta B(t) \Delta B(t+\tau) \rangle$$

One verifies that

$$\langle B^2 \rangle_w \sim \omega^{-\alpha} \tag{1}$$

with $\alpha = 2H - 1$. For a white noise case, $\alpha = 0$ and $H = 1/2$ corresponding to a WBM (Fig. 3). The spectral density is equivalent to a white noise:

$$\langle B^2 \rangle_w \sim w^0 \sim f^0$$

One can also obtain a white noise for a mutli-fractal WBM (Fig. 4).
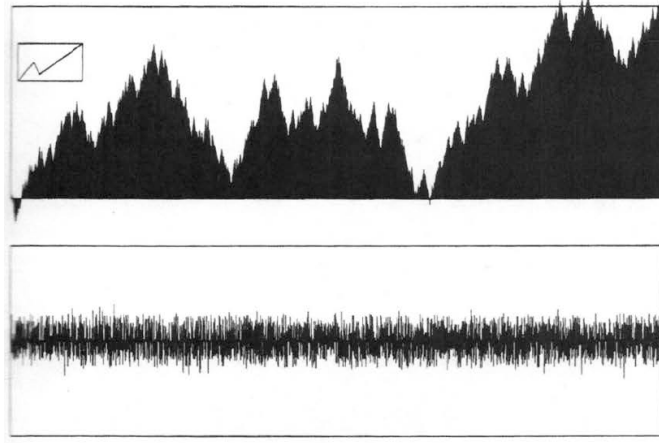
Figure 3: Top: Cumulative increments of a WBM. Bottom: Individual uncorrelated increments corresponding to the same WBM with a white noise signature.
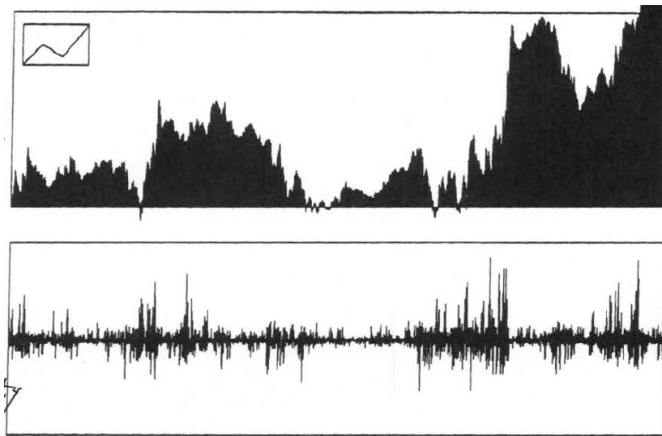
Figure 4: Top: Cumulative increments of a multi-fractal WBM. Bottom: Individual increments corresponding to the same multi-fractal WBM with a white noise signature. Here the increments are far from being Gaussian.

4 Pink noise or 1/f noise

When $H = 1$, the value α is equal to 1 and the spectral density equation is inversely proportional to the frequency, that is: $\langle B^2 \rangle_\omega \sim 1/\omega \sim 1/f$. This universal $1/f$ power law was studied by Montroll and Schlesinger in their work entitled 'On 1/f noise and other distributions with long tails'. Qualitatively, $1/f$ noise refers to a persistent distribution of events where big ones are rare and smaller ones occur much more frequently (Joseph and Noah effects). Unlike the Brownian case where fluctuations are completely random, the data points of the series have a sense of long term memory associated with the H value being equal to or close to unity. When this law occurs in electronics, it is referred to as Flicker law. A notion of self similarity and scale invariance is associated with this phenomenon.
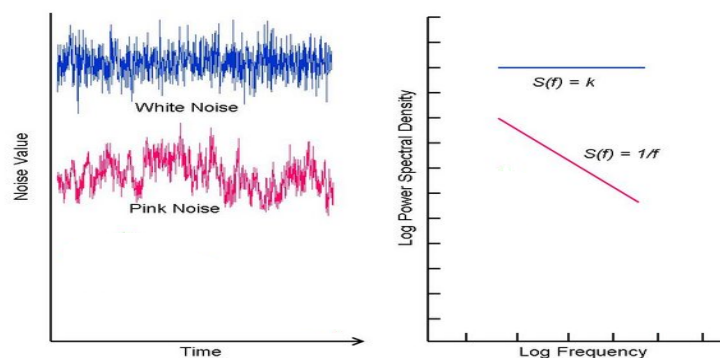
Figure 5: White and Pink noise and their corresponding spectral densities.

Although similar to Zipf's law, $1/f$ noise and the latter are not the same. In its original form, Zipf's law originated as a result of the linguistic G. Zipf trying to verify that the occurrence or appearance frequency of a word is inversely proportional to its rank in the frequency table. Population ranks of cities in different countries i.e. formation of mega cities follows a Zipf's law. Given a set of Zipfian distributed frequencies, sorted from most common to least common, the second most common frequency will occur $1/2$ as often as the first. The third most common frequency will occur $1/3$ as often as the first. The n-th most common frequency will occur $1n$ as often as the first. Although this might infer a strong similarity with the $1/f$ power law, this correspondence cannot hold exactly, because items (words in the original form of Zipf's law) must occur an integer number of times; there cannot be 2.5 occurrences of a word. Nevertheless, over fairly wide ranges, and to a fairly good approximation, both related are related.
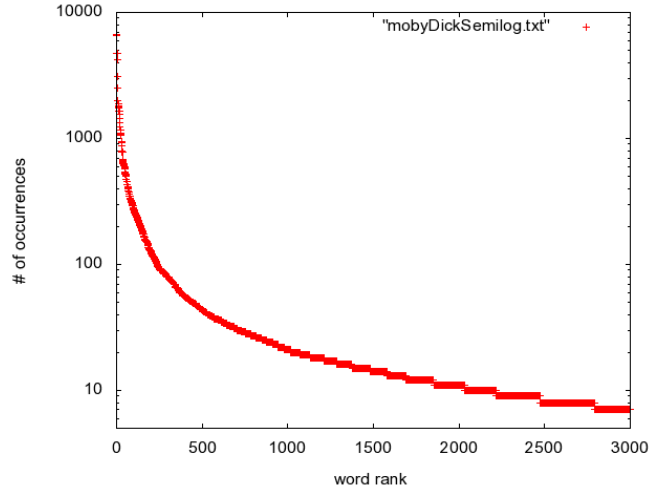
Figure 6: Zipf's law.

In the same paper referred to above, Montroll and Schlesinger tried to answer the following question: What kind of relation exists between a log-normal process and the $1/f$ power law? They considered a distribution function which logarithm $log(x)$ is normally distributed:

$$F(log(x)) = \frac{exp[-(log(x) - log(\bar{x})^2/2\sigma^2]}{(2\pi\sigma^2)^{1/2}} \tag{2}$$

$\bar{x}$ is the mean and σ^2 is the variance. Since $dlog(x) = dx/x$, the probability that the variable $x/\bar{x}$ lies in the interval $d(x/\bar{x})$ at $x/\bar{x}$ is:

$$g(x/\bar{x})d(x/\bar{x}) = P(log(x))\frac{dlog(x)}{dx} = \frac{exp[-(log(x/\bar{x}))^2/2\sigma^2]}{(2\pi\sigma^2)^{1/2}}\frac{d(x/\bar{x})}{(x/\bar{x})}$$

7

Taking the logarithm of the g expression:

$$log(g(x/\bar{x})) = -log(x/\bar{x}) - [log(g(x/\bar{x}))]^2/2\sigma^2 - \frac{1}{2}log(2\pi\sigma^2)$$

the last term being a constant. If we set $1/f = x/\bar{x}$, we can rewrite the last equation as:

$$log(g) = -log(f) - \frac{1}{2}(\frac{log(f)}{\sigma})^2 - \frac{1}{2}log(2\pi\sigma^2) \qquad (3)$$

For $\sigma \gg 1$, the relation $g = 1/f$ follows from the linear equation. On the other hand, for $\sigma \sim log(f)$ we have $g(f) \sim 1/f \sim 1/(x/\bar{x})$. This shows that the log-normal law can be well approximated by $1/f$ law.

B. Carreras, Ph. Van Milligan and C. Hidalgo investigated long range correlations of plasma edge fluctuations in different confinement systems. In ref. [1], using the ion Larmor radius ρ_i and the micro-instability inverse growth rate as scales of turbulence, l_c and τ_c respectively, the authors tried to characterize transport in plasmas by examining those long range dependences. They started by analyzing values of the Hurst exponent of the plasma edge density fluctuations as generated by a Langmuir probe. H values were found to range between 0.62 and 0.75 for three stellarators and one tokamak. Being greater than 0.5, these values are evidence of long range (persistent) correlations in the plasma turbulence; that is Mandelbrot's Joseph effect.
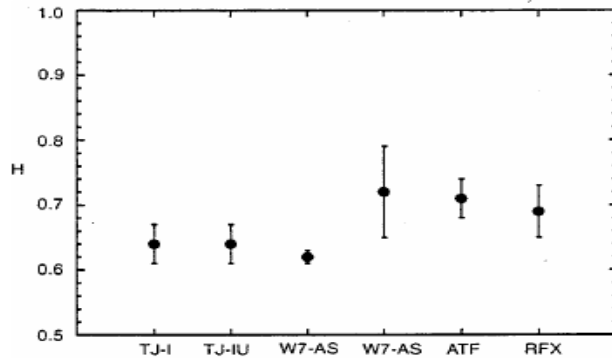
Figure 7: Hurst coefficient values for three stellarators (TJ-IU,W7-AS and ATF) and the TJ-I tokamak.

The authors also pointed out that one feature of turbulence induced fluxes is that they are bursty. In fact a probability distribution function of these fluxes shows a long tail with 10% of the largest flux events being responsible for 50% of the transport (See fig.(7) in ref [2]). This realizes Mandelbrot's Noah effect and suggests similarity with the heavy tailed Pareto distribution function to be discussed shortly.

When computing the frequency spectra of plasma edge ion saturation current, Carrers *et al.* obtained the following curve (See fig.(8)). Similar curves were obtained for the electrostatic potential fluctuations and the turbulent particle flux frequency spectra respectively. The generic form of
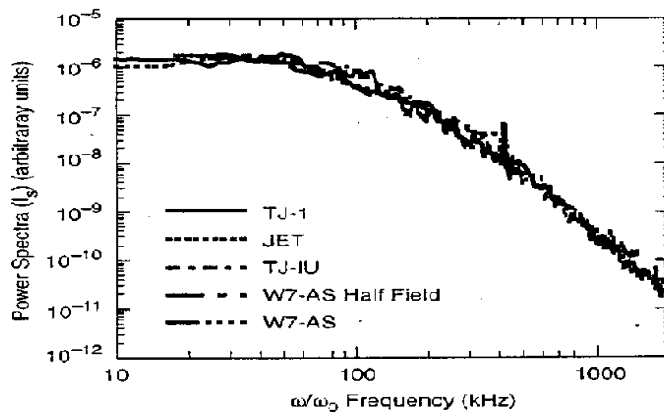
Figure 8: Frequency spectra of fluctuations in various confinement systems as function of the frequency w.

the power spectrum was found to be:

$$P(\omega) \sim \omega^{-\alpha}$$

with α being the decay index. A distinction between three regions, depending on the value of the frequency was made. For low frequencies ω, the coefficient α is equal to 0. For intermediate frequencies $\alpha = 1$ and an avalanche along with a $1/f$ noise are observed. Finally, at high frequencies, $\alpha > 3$ and a signature of a power law $\propto 1/\omega^{\alpha}$ is observed.

5   Pareto-Levy distributions and Levy flights

For systems with $H \neq 0.5$, a Gaussian probability distribution function cannot be used as a characteristic pdf. One should therefore look for an alternative distribution function to characterize these systems. Levy flights for instance, are a prime example of such systems and are characterized by a heavy tail pdf.

P. Levy was the first to study these systems along with their corresponding probability distribution functions. Motivated by the allocation of wealth, Pareto continued his predecessor work and stated the 80-20 rule which says that 20% of the population controls 80% of the wealth. Recent studies have shown however that it is more of a 70-30 rule. Regardless of percentages, the Levy- Pareto distribution is characterized by a heavy tail. In fact data

9
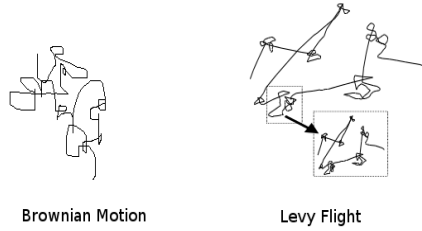
Figure 9: Brownian and Levy Flight motion.

provided by the IRS proves that the income of a great percentage of the population has an excellent fit to a heavy tail log normal distribution with the last and rare 2-3 percentile of the population accumulating wealth via means that are not available to the rest of us. B. Mandelbrot, who continued Pareto's work, investigated the survivor function of the distribution of step sizes U derived from Pareto distribution of income:

$$P(U > u) = \begin{cases} 1 & : u < 1 \\ u^{-D} & : u \geq 1 \end{cases}$$

Here D is a fractal dimension parameter and the distribution is a particular case of the heavy tail Pareto distribution (power law) with a tail index α. Initially motivated by the study of wealth distribution as we said, Pareto found that the probability of an income U to be greater than u has the general form:

$$P(U > u) = \begin{cases} 1 & : u < U \\ (u/U)^{-\alpha} & : u \geq U \end{cases}$$

for which corresponds the heavy tailed strong Pareto law:

$$p(u) = -dP(U > u) = \begin{cases} 0 & : u < U \\ \alpha(U)u^{-(\alpha+1)} & : u \geq U \end{cases}$$

Here U is a scaling factor and α is the tail index $0 < \alpha < 2$. When $1 < \alpha < 2$, the distribution is called a **strong Pareto distribution**. The negative exponent of u suggests a strong power law that leads to a slow decrease of the Pareto distribution for large u values, and the log-log plot of $p(u)$ vs u is a straight line with a negative slope.

The strong Pareto law however is acknowledged to be empirically unjustified. On the contrary, there is little question on the validity of another similar law for sufficiently large values of u. The best way of taking care of this

10

limitation is to say that $P(U > u)$ behaves like $(u/U)^{-\alpha}$ as $u \to \infty$. This defines a **weak Pareto law**

$$P(U > u) = [1 + e(u)](u/U)^{-\alpha}$$

where $e(u) \to 0$ when $u \to \infty$. Its corresponding probability density function is

$$p(u) \propto (u/U)^{-(\alpha+1)}$$

and is also characterized by a heavy tail index ($\alpha < 2$).

One might also think of the **continuous** Pareto distributions as the **discrete** counterpart of Zipf's distributions, sometimes called zeta distributions. Another example of a heavy tail distribution is the Cauchy distribution for which

$$p(\Delta x) = \frac{A}{B + \Delta x^2}$$
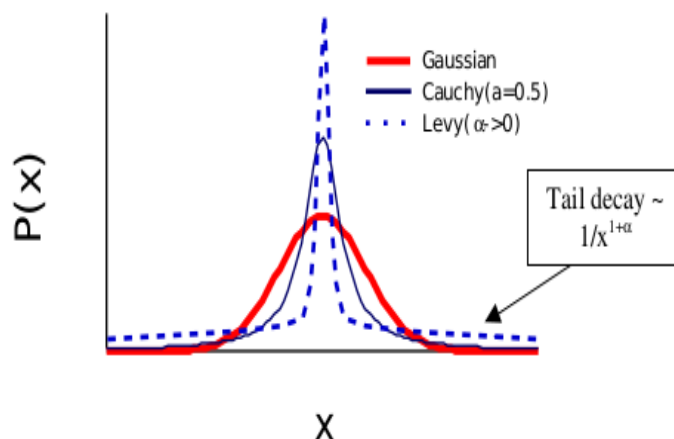
Figure 10: Comparison of tails for the three distribution functions.

The weak Pareto distribution covers only a part of the total population. In an attempt to rectify this discrepancy between the real population and that predicted by weak Pareto law, one can suggest an exponential tail distribution $p(u) \propto u^{-(\alpha+1)}e^{-bu}$ where b has to be small for $p(u) \to 0$ for large u values. Another alternative might be to work with a log-normal law since both distributions are represented by a straight line for large u values. One can then speak of $log(u)$ additivity and convergence of second order moment. These two alternatives have the same behavior as Pareto distribution with a variance that diverges for large u without any restriction on α.

6 Generalizing the Central Limit Theorem

6.1 Definition of the Levy stable distribution

Definition of Levy stability

If U' and U'' are two statistically independent incomes or samples that follow a Pareto-Levy distribution, then $U' \oplus U'' = (a'U' + b') \oplus (a''U'' + b'') = aU + b$ will also follow a Pareto-Levy distribution if all coefficients are positive. In other words, a distribution is said to be Levy-stable if a linear combination of two independent copies of a random sample has the same distribution. Gaussians, which are the only stable distributions with finite variance, and Cauchy distributions are examples of stable functions. In addition, Pareto-Levy distribution, for which $1 < \alpha < 2$, is a Levy stable process. Its density $p(u)$ is determined by its Laplace transform:

$$G(b) = \int_{-\infty}^{+\infty} e^{-bu} dP(u) = \int_{-\infty}^{+\infty} e^{-bu} p(u) du = exp[(bu^\star)^\star + Mb]$$

where $1 < \alpha < 2$, $u^\star$ is a scaling parameter and M is the expectation value.
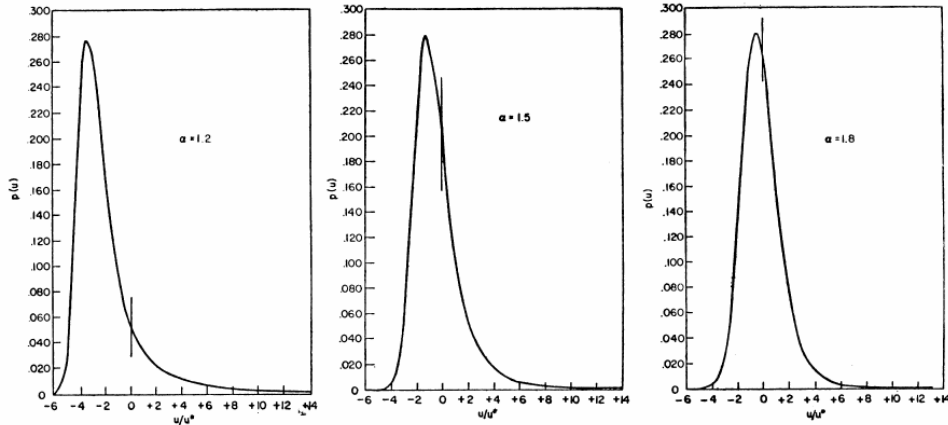
Figure 11: Densities of Pareto Levy distributions for $M = 0$, and $\alpha = 1.2, 1.5, 1.8$ respectively.

From the pictures above, one notices that as long as α is not close to 2, the P-L distribution curve very rapidly becomes indistinguishable from a strong Pareto curve of the same α. As for large negative values of u, the corresponding L-P probability rapidly decreases as $u \to \infty$, even faster than in the case of a Gaussian distribution. When α approaches 2, the P-L density tends toward a Gaussian density. Close to the limit, the P-L already resembles a Gaussian and only for large u is the Gaussian decrease replaced by a Paretian decrease.

The Central Limit Theorem states that the arithmetic mean of a sufficiently large number of independent Gaussian random variables is approximately normally distributed, regardless of the underlying distribution. This unique property of the Gaussian distribution was reconsidered by Levy who formulated a broad approach valid for distributions with infinite variance.

Starting with a normalized pdf $p(x)$ of a random variable $\int p(x)dx = 1$ and its characteristic function:

$$p(q) = \int dx e^{iqx} p(x)$$

one can write the second moment

$$\langle x^2 \rangle = \lim_{q \to 0} [-i^2 \frac{\partial^2}{\partial q^2} p(q)]$$

We look for a general form of a stable distribution that is an attractor of motion. Consider two stable distribution functions X_1 and X_2 and their linear combination $Cx_3 = C_1 x_1 + C_2 x_2$. X_3 is stable if the coefficients C_1, C_2 and C are all positive (from the stability definition stated above). If this equality holds, then the probability $p(x_3)$ for a value x to fall in the $x_3, x_3 + dx_3$ range is:

$$p(x_3)dx_3 = p(x_1)p(x_2)\delta(x_3 - \frac{C_1 x_1 + C_2 x_2}{C})dx_1 dx_2$$

Replacing the expression of $Cx_3 = C_1 x_1 + C_2 x_2$ in the generating function expression, we obtain:

$$
\begin{aligned}
p(Cq) &= \int dx_3 e^{C.\frac{C_1 x_1 + C_2 x_2}{C}} p(x_3) \\
&= \int dx_1 e^{iqC_1 x_1} p(x_1). \int dx_1 e^{iqC_1 x_1} p(x_1) \\
&= p(C_1 q)p(C_2 q)
\end{aligned}
\tag{4}
$$

that is
$$log(p(Cq)) = log(p(C_1 q)) + log(p(C_2 q))$$

The last two equations involve functions with an evident solution

$$log(p_\alpha(Cq)) = (Cq)^\alpha = c^\alpha e^{-i\frac{\pi}{2}\alpha(1-sign(q))}|q|^\alpha$$

where the exponential expression introduces a phase shift and where $C^\alpha = C_1^\alpha + C_2^\alpha$. Thus the characteristic function of a Levy distribution is

$$p_\alpha(q) = exp[-C|q|^\alpha] \tag{5}$$

with $0 < \alpha \leq 2$ to guarantee a positive characteristic function.

For $\alpha = 2$, we recover the Gaussian distribution. For $\alpha = 1$, we recover the Cauchy distribution where the Fourier transform of the exponential expression gives a Lorentzian and generates a characteristic function:

$$p_1(x) = \frac{c}{\pi} \cdot \frac{1}{x^2 + c^2}$$

An important case is the asymptotic behavior at large $|x|$:

$$p_\alpha(x) \sim \frac{\alpha C}{\pi} \cdot \Gamma(\alpha) . sin(\frac{\pi\alpha}{2}) \frac{1}{|x|^{\alpha+1}}$$

that has a heavy tail for $\alpha < 2$. The distribution behaves like a Pareto law for which:

$$p_\alpha(x) \sim 1/|x|^{\alpha+1}$$

The nth order moment, $\langle x^n \rangle = \int dx x^n p_\alpha(x)$ diverges for $n > \alpha$, that is $\langle x^2 \rangle = \infty$ preventing us from constructing a Fokker-Planck theory and using the large number law and the Central Limit theorem for $\alpha < 2$.

6.2 Levy process

The Levy process, which can be viewed as a generalization of the diffusion process, is time dependent and that has a Levy distribution at infinitesimal times Δt. Writing the probability density equation while considering a stationary state and many small steps, the result will be a Levy transition where the probability of transition from $(x_0, t_0) \longrightarrow (x_N, t_N)$ is:

$$p(x_0, t_0; x_N, t_N)$$
$$= \int dx_1 \ldots \int dx_{N-1} . p(x_0, t_0; x_1, t_1) . p(x_1, t_1 | x_2, t_2) \ldots p(x_{N-1}, t_{N-1}; x_N, t_N)$$
(6)

according to Chapman Kolmogorov equation that relates the joint probability distributions of different sets of coordinates on a stochastic Markovian process.
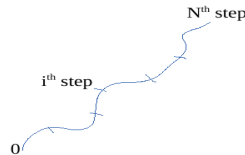
Defining $\Delta t = t_{i+1} - t_i$ and $N\Delta t = t_N - t_0$ for $N \gg 1$ and assuming the process is stationary in time and space i.e.

$$p(x_i, t_i; x_{i+1}, t_{i+1}) = p(x_{i+1} - x_i; t_{i+1} - t_i) = p(x_{i+1} - x_i; \delta t) \qquad (7)$$

Eq.(6) becomes:

$$p(x_N - x_0; N\Delta t) = \int dy_1 \ldots dy_N p(y_1; \Delta t) \ldots p(y_N; \Delta t) \qquad (8)$$

where $y_i = x_{i+1} - x_i$. When introducing the generating functions

$$p(q) = \int e^{iqx_j} p(x_j; \Delta t) dx_j$$

and

$$p_N(q) = \int e^{iqy^N} p(y^N; N\Delta t) dy^N$$

for $y^N = \sum_{i=1}^N x_i = x_N - x_1$, we finally obtain

$$p_N(q) = (p(q))^N \qquad (9)$$

Writing $p(q) \to p_\alpha(q; \Delta C)$ and $p_N(q) \to p_\alpha(q; C_N)$, these equations are consistent with Eq. 5 for a value of C_N:

$$C_N = N\Delta C = N\Delta t(\Delta C/\Delta t) = CN\Delta t = Ct$$

Therefore

$$p_N = p_\alpha(q, Ct) = exp[-CN\Delta t |q|^\alpha] \qquad (10)$$

and the characteristic function $p_\alpha(q, t)$ of the Levy process is:

$$p_\alpha(q, t) = exp[-Ct|q|^\alpha] \qquad (11)$$

To get the original Levy process, we inverse Fourier transform the previous equation and find $p_\alpha(x, t)$:

$$p_\alpha(x, t) = \int dq e^{iqx - Ct|q|^\alpha} \qquad (12)$$

The asymptotic behavior for $|x| \to \infty$ follows a power law $(p_\alpha(x, t) \sim t/|x|^{\alpha+1})$ with a long tail and one can verify that the second moment $\langle x^2 \rangle \to \infty$ for $\alpha < 2$ at any time t.

Here again the particular case of $\alpha = 2$ generates a $p_2(q) = exp[-Ctq^2]$ and a probability distribution function $p_2(x, t)$:

$$p_2(x, t) = \int e^{-iqx} . e^{-ctq^2} dq = \frac{e^{-x^2/Ct}}{\sqrt{Ct}} \qquad (13)$$

which is a diffusion propagator.

7   Realizing Levy flights in transport in fluids.

In a typical diffusive process, particles intermingle as a result of their natural random movement with a mean squared displacement $\langle (\delta x)^2 \rangle$ that is $\propto t$. There exists however anomalous processes for which the mean squared displacement is proportional to a t^γ with $\gamma \neq 1$. Depending on the value of γ, the process is said to be:

- super diffusive for $\gamma > 1$

- sub-diffusive for $\gamma < 1$

Sub-diffusion occurs in fluids with sticking regions that retard the motion of particles. For example a time dependent flow might be responsible of delaying the particles motion, making them stick to certain well defined regions. Trajectories are then chaotic. On the other hand, a super diffusive regime is characterized by particles undergoing long Levy flights which are characterized by divergent second moments as we saw above. This type of anomalous transport was experimentally studied in [3]. The experimental setup is an annular rotating tank filled with water. Water was continuously pumped inside and out of the tank from its bottom while maintaining a laminar velocity field in the rotating tank. As a result of the Coriolis force action on the pumped fluid, a sheared counter-rotating azimuthal jet is created leading to appearance of a chain of vortices or rings that move around the annulus. Passive tracers were then injected in the flow and followed along the cross section. It was found that despite the flow remaining laminar, the tracers follow chaotic trajectories, intermittently sticking to the vortices areas then moving larger distances in the jet regions that sandwich the observed six vortices. Trajectory points are collected and used to calculate the variance of the displacement of tracer particles and the sticking and flight time probability distributions. In Fig. 13, the flat parts of the θ profiles correspond to oscillatory movement of the tracer within the vortex ring while the steeper parts represent a Levy flight i.e. a transition from one ring to the other. Note that most of the transition occur in the corotating direction (positive slope) as a result of the curvature of the system. Plotting the displacement variance $\langle (\theta - \langle \theta \rangle)^2 \rangle$ versus time on a log log scale, an almost linear curve with a slope $\gamma = 1.6$ was found.

[h] $\gamma > 1$ indicates a super-diffusive regime. By computing the duration of those sticking/transition events, a pdf can be determined. An inverse power relation $P \sim t^{-\beta}$ is found for the probability distribution function of both sticking and flight times. All the previous characteristics are absent when the experiment is repeated in a turbulent flow. As a final outcome, the experiment is a proof of anomalous transport and Levy flights in fluids that clearly illustrates Madelbrot's Joseph effect (oscialltory movement), that gets interrupted Madelbrot's Noah effect (Levy flights from one ring to the other).
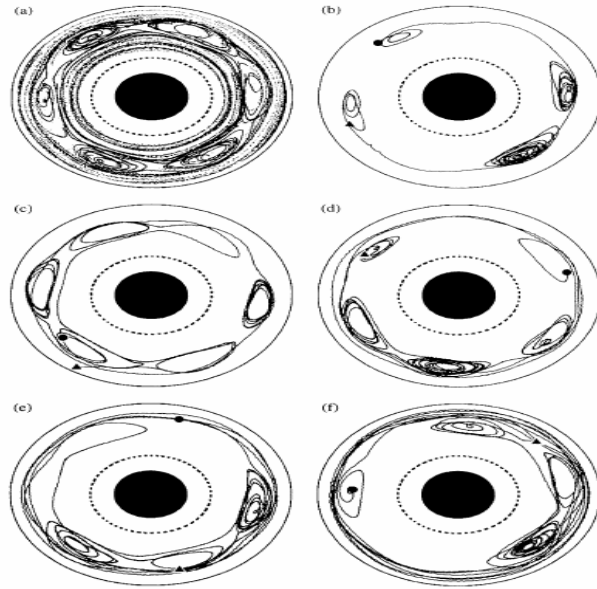
Figure 12: Vortices and time evolution of trace particles in a rotating tank.
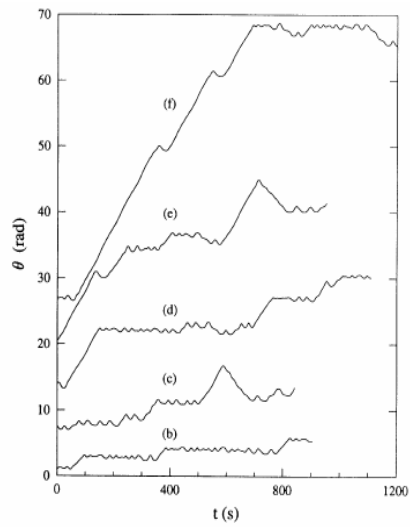
Figure 13: Azimuthal displacement as function of time.
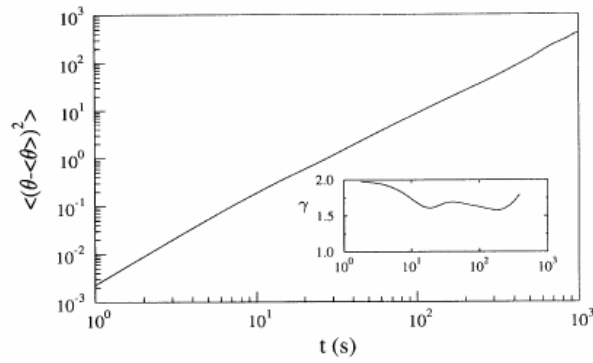
Figure 14: Variance of the azimuthal displacement vs. time.
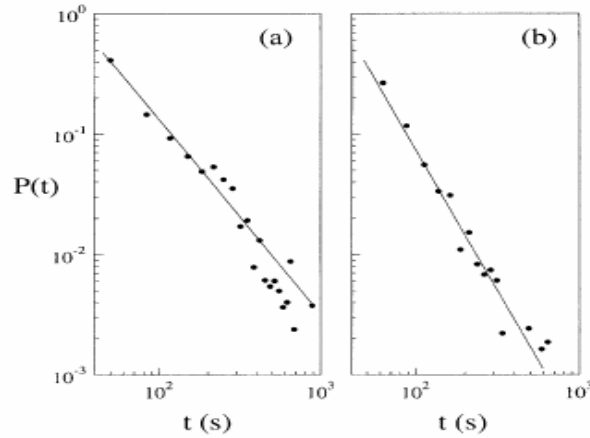
Figure 15: a) Sticking time pdf exhibiting a power law with a negative slope $\gamma = 1.6$. b) Flight time pdf exhibiting a power law with a negative slope $\mu = 2.3$

References

[1] B. A. Carreras, B. Ph. van Milligen, M. A. Pedrosa, R. Balbin, C. Hidalgo, D. E. Newman, E. Snchez, R. Bravenec, G. McKee, I. Garc??a-Corts, J. Bleuel, M. Endler, C. Riccardi, S. Davies, G. F. Matthews, E. Martines, and V. Antoni. Experimental evidence of long-range correlations and self-similarity in plasma fluctuations. Physics of Plasmas, 6(5):1885–1892, 1999.

[2] M. Endler and et al. Nuclear Fusion, 35:1307, 1995.

[3] T. H. Solomon, Eric R. Weeks, and Harry L. Swinney. Observation of anomalous diffusion and lévy flights in a two-dimensional rotating flow. Phys. Rev. Lett., 71:3975–3978, Dec 1993.